

Article

Integrated Economic Optimization of Hybrid Thermosolar Concentrating System Based on Exact Mathematical Method

Stylianos A. Papazis 

Department of Electrical and Computer Engineering, School of Engineering, Democritus University of Thrace, 67100 Xanthi, Greece; spapazis@ee.duth.gr; Tel.: +30-25410-79938

Abstract: This article presents an integrated approach for solving the optimization of economic dispatch and commitment EDC problems of hybrid thermosolar concentrating power generating systems using matrix mathematics. The model uses matrices, and is solved by matlab programming. The study case of a hybrid thermosolar system in the north-west of Greece shows the impact of concentrating solar power (CSP) generation on the optimal cost of energy produced: the CSP system increases the operational costs as compared to the fossil fuel thermal systems. To acquire the benefits of cleaner electric energy with diminished emissions versus the minimal cost of electrical energy generation belongs to multicriteria managerial decisions. This approach can be applied to hybrid energy systems with large numbers of thermal and CSP generators. It offers an accurate instrument to energy engineers and researchers, for critical managerial decisions regarding electrical energy economics.

Keywords: concentrating solar systems; economic optimization; energy economics; hybrid energy systems; renewable energy



Citation: Papazis, S.A. Integrated Economic Optimization of Hybrid Thermosolar Concentrating System Based on Exact Mathematical Method. *Energies* **2022**, *15*, 7019. <https://doi.org/10.3390/en15197019>

Academic Editor: Maria G. Ioannides

Received: 12 August 2022
Accepted: 14 September 2022
Published: 24 September 2022

Publisher's Note: MDPI stays neutral with regard to jurisdictional claims in published maps and institutional affiliations.



Copyright: © 2022 by the author. Licensee MDPI, Basel, Switzerland. This article is an open access article distributed under the terms and conditions of the Creative Commons Attribution (CC BY) license (<https://creativecommons.org/licenses/by/4.0/>).

1. Introduction

The integration of electricity generated from renewable energy sources (RES), such as from wind and solar, into hybrid grids supplied by thermal power units, and the variability of RES, impacts the generation dispatch. The generation scheduling problems take into consideration the variability and nondispatchable characteristics of RES because of their random nature: solar irradiation and wind velocity are undefined, and their availability is not related to the load demand. Effective strategies for covering the increasing energy demand while attaining greenhouse emission reductions are to integrate RES in various existing power grids [1–4]. The re-engineering and retrofit of power plants to integrate RES are linked to the necessity to supply demanded amounts of power to the electrical grid. Some benefits of hybrid grids with integrated RES are decreasing the use of thermal generation units, impacting load dispatch and providing environmental advantages [5].

The technologies of concentrating solar power CSPs and photovoltaics PVs convert solar into electrical energy. In 2019, the expanding installations of PVs were at 578 GW while the installations of CSPs were at 6 GW, and this led to cost declines of solar systems, resulting that the 40% of the solar installations had lower costs than the fossil fuel generating systems [6].

The variation of solar irradiance due to cloud shadowing produces variations in generation of power, which can have effect on balancing the load demand and the generated reserves. Even on a day without clouds between sunrise and sunset, the electric energy generated from all the solar units of the system fluctuates.

Solar energy combined with lignite resources forms a solar aided power generation SAPG system, which is a hybrid plant of thermal and solar energy-based powerplants. One of the benefits of integrating such thermosolar systems into existing lignite power plants

and retrofitting the existing infrastructure to implement a hybrid concentrating solar power CSP system is that the generated electrical power is not influenced by sunshine.

On the other hand, managerial and political decisions, taking into consideration unexpected events in society, such as the recent pandemic COVID-19, or war conflicts, or energy crises, try to balance the effects of shortages of fuel resources by importing, or by locally available raw materials, and switching from unavailable resources. The impact is that the cost of electric energy fluctuates and the forecasting of ceilings prices become difficult. In this context, the coal resources are reconsidered for supplying the available existing thermal generating units, or new ones that will be built in the near future [7]. One example is the lignite power plants located in the northwest of Greece: at Amideo, Ptolemaida, Kardias, and Agios Dimitrios. In the context of prioritizing environmental criteria, some thermal power plants lowered or stopped their operation, while other units with alternate supplies undertook the load commitment. In the new situation of the pandemic and war conflicts, the imports of raw fuels diminished and attention was switched back to lignite resources [7]. Following this, emerged the need to deeply study the hybrid thermosolar generating systems, together with the related economic aspect.

In the operation of power systems must be implemented an optimal economic dispatch and commitment EDC, which concern the optimization of power generation by installed units, the optimization of an objective cost function and the optimization of the total fuel cost, with power balance and other operational constraints. The solutions accomplish the dispatch of generation units, takes into consideration the constraints, and optimize the total operational cost [8,9].

Optimization of EDC has attracted attention and developed well-organized new techniques, some remarkable are implemented with Lagrange multipliers theory. The new applications need new models and algorithms, that can be easily used by specialists. The EDC problem are multifaceted because of the large number of generators connected to hybrid grids, each one with constraints, which jointly form objective cost functions. Thus, optimizing the task of dispatching the available generating units to generate electrical energy, optimizing their costs, and studying the electricity production in hybrid power networks, is recently receiving consideration [10].

In the last decades, emerging technologies influenced energy engineering education too [11,12]. For this reason, academics undertook to teach technological innovations and to sustain the future careers of graduates, by helping them to develop innovative skills [13]. Such skills of graduates will be passed on to society, by involvement of parents and relatives in the knowledge and use of new technologies. Because the introduction of new technologies in teaching and research continues to be in transition, they should be considered in the methods of learning [10–14].

The EDC software used by energy companies is not available; it cannot be accessed for educational purposes because of the high cost, while existing classical software, which handles limited numbers of generators and programs for EDC does not run on newer computers, or operating systems [14]. Sometimes, publications present solved applications, with few generating units and selected cost functions characteristics that converge easily, and conclude that EDC problems are easy. Other publications based on equations from references, report results, but without giving details on how to solve EDC problems. Instead of finding details about the solutions, the readers are directed to search for other publications, which also are based on other references, etc. From consecutive retrieving, and reusing of information, the measurement units for variables do not match, or are in different currencies, or parity rates for currencies are not reliable in the time of the study, or symbols used in the equations are not defined, or symbols have different meanings from author to author. Publications report study cases solved by using toolboxes from commercial software, where must input the data, and choose the solution. From the investigation of methods, and techniques for EDC optimization in hybrid energy systems, we found a large amount of literature related to optimal control, and computer software, while the economics' aspect which is the main topic remains in the backyard. From researchers' point

of view, because of the lack of consistency, such categories of publications cannot be used to continue research, or follow-up, or base new findings.

To bridge the gaps, this paper developed an integrated approach for hybrid thermosolar concentrating systems for EDC optimization, based on exact matrix mathematics, which can be used as a research tool for multicriteria economic management decisions. This approach solves the optimal EDC problem of a hybrid thermosolar system, which comprises thermal generators and CSP systems. The problem of optimizing a CSP plant presumes that RES is influenced by solar irradiation, climate factors, geographical coordinates, and the month of the year. To address this issue, to the model of thermal generation from [10] is added the solar generation unit, and the model was extended to solve the economic dispatch and commitment versus time of hybrid thermosolar CSP systems.

The paper is organized as follows: Section 2 presents a review of the literature; Section 3 presents the EDC problem formulation and the methodology for an optimal solution of the hybrid thermosolar CSP system; Section 4 presents the study case of a hybrid thermosolar power system in the northwest of Greece, with varying load demand and solar irradiation distribution on an hourly basis for 24 h; Section 5 presents the results and discussion; the concluding remarks are in Section 6.

2. Literature for Hybrid Thermosolar Systems and EDC Optimization

The introduction of RES for energy generation and the diminishing of CO₂ emissions is tackled in many articles in the literature [15,16]. The transition towards sustainable energy systems includes the development of new technologies for energy generation, from fossil-based to zero-carbon, which reduce CO₂ emissions and limit global warming effects and develop new power plants based on RES [17–19].

The energy transition with increased penetration of RES uses information technologies, energy market mechanisms, and needs clean energy policy frameworks [20]. A review of the literature on the exploitation of RES, with a focus on technologies, availability, and research is in [21]. The literature studied wind, solar heating-cooling, wave power, geothermal energy, and electric energy generating technologies, and assessed their grid integration, and environmental issues. Other published information on solar energy, biomass, biogas, transition issues, design of new RES systems, investments' strategies are summarized in [22].

Parabolic trough PT systems, accomplishing thermal energy collection, are of the first commercially effective CSP technologies. As of 2018, 90% of the CSPs in operation were PT plants. Recent trends of CSP technology are: (a) R and D on the key components, and research on the overall performance to study detailed parameters, through modeling, simulation, and experiments, and (b) transition from one technology to multiple technology energy systems, such as a hybridization of solar thermal power and photovoltaic power generation [23].

Thermal power plants implement a regenerative Rankine cycle. By using PTs, the solar energy is introduced in thermal power plants to preheat water and replace the heat produced by coal [24]. To increase the efficiency, part of the steam from the turbine preheats the water feed to boiler. The SAPG uses solar energy to replace the extracted steam in the Rankin cycle, while the saved steam generates power. Two operation modes are: (a) the power boosting, where the plant consumes a constant amount of fuel while the steam produces additional power, and (b) the fuel saving, where the plant consumes less fuel, while the power output is constant. The solar irradiation received by the PT by using the mirrored surface of the linear parabolic mirror is reflected to the receiver, then sent to the absorber installed inside the receiver, thus producing its heating. The heat is sent to thermal liquid, which flows into the absorber and is directed to the heat exchanger, thus the water is transformed into superheated steam. The steam rotates the turbine connected to the electric generator. Paper [24] presents the combination of thermal with solar energy into one thermal power plant, where the solar energy replaces part of the extracted steam, thus reducing the consumption of coal. The paper studies different scenarios for SAPG, for the lignite power plant with PT solar collector field.

In the literature there are studies of solar systems and SAPG energy. An example is the model of a hybrid PV system with a solar concentrator and a heat-recovery interface [25]. The model of PV module includes the temperature gradients in the cells, and the temperature variation is predicted from the cooling strategy. The in-home energy management controllers offer solutions for maintaining comfort and providing lower bill costs and reduced CO₂ emission. The management and scheduling of electric energy consumption for controllable heating, and the amounts received from sun and wind, are studied in [26]. The aim is an efficient integration of RES, for the better energy management, to reduce the costs, and emissions. Electricity bill reduction can be realized by installing a management controller which implements the hybrid algorithms for integrating RES, scheduling the power consumption, and shifting the load demand from high to low-peak hours.

The advantages of PT over flat-plate collectors, and the design parameters of a PT collector system are presented in [27]. The effect of solar energy on the performance of PT thermal power plants with steam, gas, and thermal storage, is described in [28]. The economic analysis studies the effect of the solar energy on the levelized cost of electricity LCOE, and on fuel consumption. The stability of voltage in a hybrid power system with PT, dish-Stirling and a diesel generator is studied in [29]. The system of dish-Stirling connected to an induction generator requires the reactive power for the magnetization, while PT solar connected to a permanent magnet synchronous generator does not require reactive power. At constant load demand, the hybrid dish-Stirling-PT solar system have reduced reactive power needs, improved voltage compensation, thus increasing voltage stability.

A solar system with PT was implemented in the Mediterranean region of Almeria, Spain, for studying the steam production with solar contribution [30]. The results of the control scheme for constant pressure and temperature of produced steam at the solar field outlet, show that changes in solar radiation influence the quantity of steam formed by the solar field. In [31] are presented two operation strategies and modes: base load production and demand coverage for integrated hybrid CSP with PT solar plants and PV systems, operating in the south of Spain. In [32] is carried out an economic feasibility study for a PT thermal power plant in Cyprus. The study considers the available data, the solar potential of Cyprus, the governmental policy for RES and the feed-in tariff. A cost-benefit analysis based on: solar thermal plant capacity, capital investment, trading prices, and CO₂ emissions, shows that under certain conditions, this installation is profitable.

The performances of the hybrid PV thermal system in Bordj-Cedria, Tunis, Tunisia, were studied in [33] using energy balance equations, the parameters of a PT collector field installed and meteorological data. The hybrid PV thermal prototype has electrical and thermal efficiencies were approximatively at 7%, and 44.38%, respectively.

Other studies on the performance of CSP plants in different areas, such as Maroc and Pakistan, are presented in [34–40]. In [41] is carried out a techno-economic feasibility study of a hybrid power system to cover the electricity demand of an isolated city, not connected to the power grid, in South-West of Algeria. The feasibility of some schemes with the RES power generation was studied and the results show that the total load demand of the city could be covered by using a hybrid system with of a wind module, a PV module and a diesel generator for backup purposes.

A review including the study of power plants in the Mediterranean region of Crete Island is presented in [42]. Results show that the power plants could produce 11.19 GWh annually, with an investment cost of approximately 27 M EUR, with a payback after 16 years of operation, and then profit after 25 years is at 25.5 M EUR. In [43] presented an economic analysis of the 300 MW lignite power plant in Ptolemais, Greece, with one solar field of PT collectors.

The integration of SAPG in a power plant with a thermal energy storage (TES) system was studied in a 330 MW power plant at Yinchuan (China) [44]. The study shows that when the SAPG plant uses TES in a controlled manner, the energy efficiency increases by 2.5% and reduces the LCOE by 0.27 cents/kWh. A model for the study of energy generated and the economic benefits of the SAPG systems, its correlation to different plant capacities, has

been developed in [45]. The study cases involved four coal-power plants located in Lhasa, Tibet, China, retrofitted into SAPG plants, with capacities of 1000 MW, 660 MW, 600 MW and 300 MW. Based on multiple criteria and indexes such as solar-to-electricity efficiency (SEE), solar power generation (SPG), saved standard coal consumption rate (SCCR), annual SEE and LCOE, the results show that the SAPG benefits depend on capacity of the coal power plant and on the collector areas installed. The results show that the annual SEE is higher in larger plants and the saved SCCR is higher in smaller plants. The application of the solar tower and PT aided coal-fired power generation systems. The plant of 600 MW in Delingha, northern Qinghai, China, was developed in [46], incorporating the predictive weather data and power load, to minimize coal consumption in a selected time horizon. Using the day simulation shows that the coal consumption reduction using a predictive control approach increases by 21.3 tons (13.6%), and by 320 tons (20.3%) in 10 consecutive days. The improvement is achieved by storing more energy in the TES, and discharging it optimally. The reduction was more significant in high solar irradiation conditions, which gave a saving of 61.7 tons (34.3%).

The optimization of ED has been studied searching for higher savings in operating cost [9,10,47]. A review of the hybrid RES including modeling, control, reliability, optimum sizing, and feasibility analysis, is presented in [48]. Reference [49] proposes an optimization model for a day-ahead schedule with RES uncertainties influencing the dispatch. Optimal scheduling by minimizing the day-ahead costs, taking into account uncertainties in wind, and solar forecasts, is proposed by [50]. A solution for ED problems results from computing the optimal power generated with the least cost using the lambda iteration method in [51]. Reference [52] examined the conditions that influence the optimality of ED, and proposed the linear programming. Publication [53] addresses the ED optimization with the prohibited operating zones and the physical operational constraints by using the lambda-iteration method. In [54] the ED is considered as a multiobjective optimization problem, and is solved by linear programming.

In [55] Lagrangian multipliers with monotonic cost functions are used for Lagrangian relaxation, and separates the large-scale optimization into smaller systems. The augmented Lagrangian relaxation with penalty term is solved using a quadratic approximation method, and decomposition into several ED models [56]. For large-scale integration of RES, ED is a dual problem of the Lagrangian relaxation [57]. In [10] is developed a generalized Lagrange multipliers with lambda iterations method based on matrix mathematics for thermal power plants, and concludes that, in the context of emerging technologies, professionals and scientists must be informed about ED management.

From the literature review results that, the optimal scheduling handles the thermal units, specifics of RES and of the load demand. In the view of the involvement of RES in the generation and forecast of load demand, the scheduling must be adapted to specific requirements. Attempts have been made in the literature, but it is required an exact mathematical method which reflects the implications of varying fuel costs, changing the operation and maintenance costs, taking into consideration the variability of RES, and solving the real-time dispatch problem. This paper bridges this gap. In the proposed optimal scheduling strategy, the varying solar power generation is estimated using the varying solar power irradiation and the varying load demands in real time.

3. Economic Dispatch and Commitment Optimization of Hybrid Thermosolar System

Power systems need management for generating units that supply the electrical load demand, considering specific technical aspects such as power-output limits, network constraints, and efficient economic management. The objective of the EDC problem is to control the production of every generating unit i in the power system where: to minimize the total costs, supply the electrical load demand, and meet the technical and security constraints [8–10].

In the followings, the optimal scheduling is expressed taking into consideration the hybrid thermosolar generation system. The power units of the hybrid system are: thermal generators with fossil fuels (lignite), and concentrating solar power CSP systems, all

connected to the power grid. The output of the CSP modules is predicted according to the geographical longitude/latitude, and month of the year, on a 24-h basis using solar tracking.

The hybrid energy system involves subsystems for the generation and consumption: thermal units, concentrating solar units, time-varying loads, external data files, and an energy management system EMS, which controls the power dispatch between generating units and load demands, during different time periods and operating situations. The EMS switches dynamically and achieves a power balance versus time, when energy sources and load demands are varying. The hybrid thermosolar system has the control system with EMS, the lignite thermal units, the concentrating solar units and varying electrical loads such as motors, elevators, heating-cooling, air conditioning, lightings, other buildings and industrial equipment, etc.

Power systems operate as energy entities, meeting the committed load needs from the already installed thermal power units (lignite, full oil, and gas technology).

The retrofit by the addition of RES, which is proposed by this research, does not aim at a complete replacement of the existing power generation systems, but acts as an adjunct to them, with the aim of weakening the emissions from the use of fossil fuels. In the situations when the power produced by RES is not enough, the balance of committed power is achieved by existent fossil fuel thermal generation units.

3.1. External Data

Sun irradiation levels are periodically varying daily, and are dependent on geographical coordinates longitude and latitude, on the days and months of the year, and consequently, depend on the location, as shown in Figure 1. The two-axis maximum point solar tracking system is considered for increased irradiance and longer duration during the day [58]. The selected geographical coordinates are of a lignite power plant from the Ptolemaida area, in northwest of Greece.

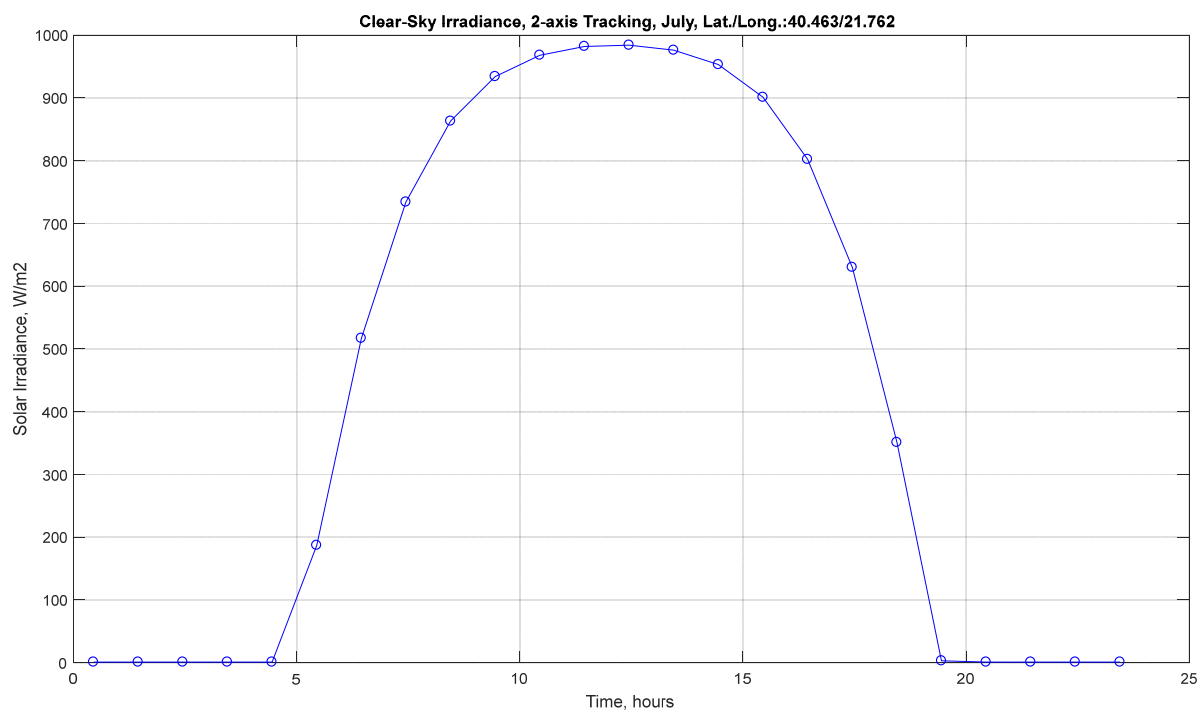


Figure 1. Solar Clear-sky irradiance, on a 2-axis tracking plane, in the month of July, at Ptolemaida, NW Greece, latitude/longitude: 40.463/21.762, during 24 h.

An estimation of varying electrical loads versus time, is shown in Figure 2. Depending on operating conditions, industrial loads such as electric motors can be connected to the

system. In our approach it is estimated that the varying electrical loads represent the $\cong 0.20\%$ of the total committed electrical load.

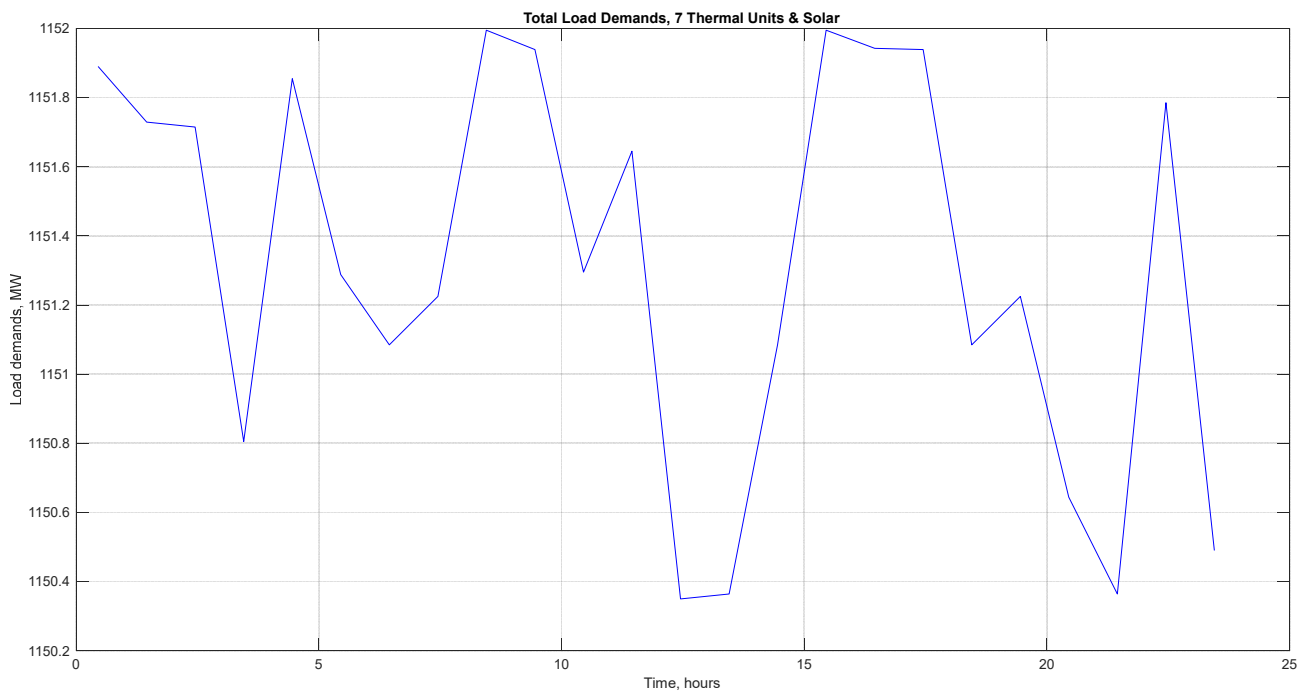


Figure 2. Estimated varying electrical load demands on a 24-h basis.

These external data files integrate: the sun irradiation, Figure 1, and the power load demands, Figure 2, which are vary over time for the period under consideration. The mathematical model uses the following data-files, as data resources (in spreadsheet format) of the external parameters: sun irradiation file, and load demands file. External data are user defined prior to the simulation in order to implement exact simulation scenarios.

3.2. Generation Constraints

We consider a number $i = 1, 2, \dots, N$ of thermal units which supply the electrical load demand, where N is the total number of thermal units. The generalized model of thermal ED optimization, developed in [10], in the present work is extended for modeling hybrid thermosolar modules, by Equations (1)–(47).

The costs of thermal units, is formulated as:

$$C_i = C_{F,i} + C_{V,i} \dots \forall i \quad (1)$$

where C_i is the total cost of thermal unit i , $C_{F,i}$ is the fixed cost, or no-load cost of thermal unit i , and $C_{V,i}$ is the variable cost of thermal unit i . An alternative to total cost is the cost rate $F_i(P_i)$ of thermal unit i , for a time interval of one hour, $t = 1$ h, where P_i is the output power of thermal unit i .

$$F_i(P_i) = C_i/t \quad \forall i \quad (2)$$

One essential constraint is the power balance, showing that the sum of the output powers P_i equals the total electrical load demand P_L , and thus, sets to zero function Φ_{th} :

$$\Phi_{th} = P_L - \sum_{i=1}^N P_i = 0 \quad (3)$$

The total power available in the network must be larger than the demand by a prespecified amount R_L which is the mandatory Reserve, or the power available in excess over the load demand P_L :

$$\sum P_{i,\max} \geq P_L + R_L \quad (4)$$

There are physical constraints on the generation levels. Thermal units do not function below a minimum power, or above their maximum capacity. The generators cannot exceed their maximum rates, $P_{i,\max}$ and also, they cannot operate below zero (otherwise they could reverse operation). All units cannot operate at zero power, and as a result, the minimum is denoted as $P_{i,\min}$. Therefore, according to [8,9], the generation limits are represented as in Equation (5), where is the power bound of each thermal unit i .

The technical constraints give $2 \cdot N$ inequalities: the power P_i is greater than or equal to the minimum $P_{i,\min}$, and less than or equal to the maximum capacity $P_{i,\max}$:

$$P_{i,\min} \leq P_i \leq P_{i,\max} \quad \forall i \quad (5)$$

The left-hand side of constraints (5) enforces that, if the power unit i is online during time period t , its power output must be above the minimum power output. This minimum power output of thermal units is generally 10% of the rated capacity of the unit [8,9]. Analogously, the right-hand side of constraints (5) enforces that if generating unit i is online during time period t , its power output should be below the maximum power output.

The penetration of solar power to system is given by [59]:

$$|P_{sk}| \leq P_{sk,\max} \quad k = 1, 2, \dots, N_s \quad (6)$$

where N_s is the number of solar collectors SC units, P_{sk} is the solar generated active power by SC unit k , and $P_{sk,\max}$ is the maximum active power generated by solar unit k , depending on solar irradiation and temperature. Thus, for the considered hybrid thermosolar system, the power balance from (3) becomes (7):

$$\Phi = P_L + R_L - \sum_{i=1}^N P_i - \sum_{k=1}^{N_s} P_{sk} = 0 \quad (7)$$

3.3. The Objective Function

Considering the EDC situation for a thermosolar energy system of N thermal units, and N_s SC units, covering a specific varying electric load demand P_L , the objective function that must be minimized is the total cost rate function F , with constraints for power bound and power balance. Thus, the EDC optimization of the objective function, in the hybrid thermosolar system is:

$$\text{Min}_F = \text{Min}_-(F_T + F_s) \quad (8)$$

$$F_T = \sum_{i=1}^N F_i(P_i) \quad (9)$$

$$F_s = \sum_{k=1}^{N_s} F_{sk}(P_{sk}) \quad (10)$$

$$F_{sk}(P_{sk}) = t_k \cdot P_{sk} \quad (11)$$

where F_T is the total operating cost rate of the system of N thermal units, $F_i(P_i)$ is the fuel cost rate function, P_i is the electric power generated by the thermal unit i , P_{sk} is the power output from the SC unit k , and t_k is the direct cost coefficient of the solar unit k . The function F_T includes fixed costs constant with the output (investment, personal, etc), and variable cost (fuels, maintenance, energy, and taxes) [8,10].

The function F_s is the direct cost of the solar power unit. If the CSP plants belong to the system operator, because the CSP power requires no fuel, the cost function do not exist, except the situations when the system operator assigns a payback cost for initial cost for the CSP plants, or assigns an operation, maintenance and renewal cost [6,59–61]. In nonutility owned CSP plants, the solar generation has a direct cost from contractual agreements. The generation of the CSPs is decided by the system operator, and bound to upper and lower limits, according to optimal operation agreements [62]. With approximation, this can be considered as analog to the scheduled CSP power, or totally neglected [63,64]. Usually, the direct cost is neglected when CSP plants are in the system utility-owned, and considered to be proportional to the scheduled output when CSP plants are nonutility-owned. In the approach of this paper, a linear cost function was used for the scheduled CSP generation [59]. Thus, the objective function can be written as:

$$F = \sum_{i=1}^N F_i(P_i) + \sum_{k=1}^{N_s} t_k \cdot P_{sk} \quad (12)$$

3.4. Thermal Energy System

The minimization of objective function F uses Lagrangian L , with constraints, and Lagrange multipliers [10,65]. Lagrangian L is formulated by adding to F , (12), the constraint Φ , (7), and multiplied by a variable lambda λ :

$$L = F + \lambda \cdot \Phi \quad (13)$$

By introducing the incremental cost rate of the thermal unit i , $\frac{\delta F_i(P_i)}{\delta P_i}$, the optimal solutions of F are obtained by setting to zero all i first partial derivatives of Lagrangian L with respect to P_i , and λ :

$$\frac{\delta L}{\delta P_i} = 0 \Rightarrow \frac{\delta F_i(P_i)}{\delta P_i} - \lambda = 0 \quad (14)$$

$$\frac{\delta L}{\delta \lambda} = 0 \Rightarrow \sum_{i=1}^N P_i - P_L + \sum_{k=1}^{N_s} P_{sk} = 0 \quad (15)$$

Thus, from (5), (12), (14), (15), according to [9,10], the necessary conditions are in (16)–(18):

$$\frac{\delta F_i(P_i)}{\delta P_i} = \lambda \quad \text{for} \quad P_{i,\min} \leq P_i \leq P_{i,\max} \quad (16)$$

$$\frac{\delta F_i(P_i)}{\delta P_i} \leq \lambda \quad \text{for} \quad P_i = P_{i,\max} \quad (17)$$

$$\frac{\delta F_i(P_i)}{\delta P_i} \geq \lambda \quad \text{for} \quad P_i = P_{i,\min} \quad (18)$$

3.5. Solar Energy System

The hourly data of the solar irradiation are required to forecast the performance of the SC unit. The power output $P_{sk}(I)$ can be controlled using solar power tracking to obtain the maximum generation of CSP. The contribution of SC unit during $\Delta t = 1$ h is:

$$P_s = \sum_{k=1}^{N_s} P_{sk}(I) \quad (19)$$

where I is the solar irradiation retrieved from external data files (in W/m^2), (Figure 1), and $P_{sk}(I)$ is the function of solar irradiation conversion to electric power of the SC unit k from the CSP system, given by:

$$P_{sk}(I) = \begin{cases} P_{sr} \left(\frac{I^2}{I_{std} \cdot I_C} \right) & \text{for } 0 < I < I_C \\ P_{sk,\max} & \text{for } I > I_C \end{cases} \quad (20)$$

where I_{std} is the reference solar irradiation set at 1000 W/m^2 , I_C is a cut-off irradiation level set at a maximum value of the considered SC 1500 W/m^2 , $P_{sk,max}$ is the equivalent power output corresponding to I_C , or the available maximum active power generated by solar unit k , and P_{sr} the rated equivalent power output of the SC, which depends on efficiency η , area S of the considered SC, and per unit base value P_{sro} :

$$P_{sr} = P_{sro} \cdot \eta \cdot S \tag{21}$$

3.6. Solution

The above problem can be solved by deducing a mathematical model with matrixes from Equations (4), (5), (7), (8), (13)–(18), and (19)–(21).

The cost rate $F_i(P_i)$ of each thermal unit i is computed from the heat rate $H(P_i)$ multiplied by the fuel cost FC_i :

$$F(P_i) = H(P_i) \cdot FC_i \tag{22}$$

The vectors of generated powers $[P]$, cost rates $[F(P)]$, fuel costs $[FC]$, the matrices of heat rates $[H(P)]$ are detailed in (23)–(28), where matrixes with dots indicate the multiplication element-by-element, and matrixes with superscripts $[x]^T$ are transposed matrixes:

$$[P] = [P_1 \ P_2 \ \dots \ P_N]^T \tag{23}$$

$$[F(P)] = [F_1(P_1) \ F_2(P_2) \ \dots \ F_N(P_{1N})]^T \tag{24}$$

$$[FC] = [FC_1 \ FC_2 \ \dots \ FC_N]^T \tag{25}$$

The heat rates $H_i(P_i)$ are quadratic (convex) characteristic functions (26), which give the following matrixes [10]:

$$H_i(P_i) = H_{i,2} \cdot P_i^2 + H_{i,1} \cdot P_i + H_{i,0} = \sum_{j=0}^2 H_{i,j} \cdot P_i^j \tag{26}$$

$$[H(P)] = \begin{bmatrix} H_{1,2} \\ H_{2,2} \\ \vdots \\ H_{N,2} \end{bmatrix} \cdot [P]^2 + \begin{bmatrix} H_{1,1} \\ H_{2,1} \\ \vdots \\ H_{N,1} \end{bmatrix} \cdot [P] + \begin{bmatrix} H_{1,0} \\ H_{2,0} \\ \vdots \\ H_{N,0} \end{bmatrix} \tag{27}$$

$$[F] = [H] \cdot [FC] \tag{28}$$

By replacing (23)–(28) in (14) and (15) we get:

$$[A] \cdot [P_0] + [B] = 0 \tag{29}$$

where:

$$[A] = \begin{bmatrix} 2 \cdot H_{1,2} \cdot FC_1 & 0 & \dots & 0 & -1 \\ 0 & 2 \cdot H_{2,2} \cdot FC_2 & \dots & 0 & -1 \\ \vdots & \vdots & \vdots & \vdots & \vdots \\ 0 & 0 & \dots & 2 \cdot H_{N,2} \cdot FC_N & -1 \\ -1 & -1 & \dots & -1 & 0 \end{bmatrix} \tag{30}$$

$$[B] = \left[H_{1,1} \cdot FC_1 \ H_{2,1} \cdot FC_2 \ \dots \ H_{N,1} \cdot FC_N \ P_L - \sum_{k=1}^{N_s} P_{sk} \right]^T \tag{31}$$

$$[P_0] = [P_1 \ P_2 \ \dots \ P_N \ \lambda]^T \tag{32}$$

The solution of (29) is in (33), and $[P_0]$ gives the initial, or the global unconstrained optimal vector of generated thermal powers:

$$[P_0] = -[A]^{-1} \cdot [B] \quad (33)$$

From $[P_0]$, we obtain the unconstrained optimal values for generated thermal powers P_1, P_2, \dots, P_N , and the Lagrange multiplier $\lambda = \lambda_1$. Vector $[P_0]$ is the optimal solution of the unconstrained system which minimizes the cost function (8). The value $\lambda = \lambda_1$ is the initial incremental cost rate, and P_1, P_2, \dots, P_N indicate the initial operating point.

λ -iteration is introduced as a small displacement $\pm\Delta\lambda$ from λ_1 . To apply the boundary conditions (5) to $[P_0]$, with the constraints (16)–(18), and introducing the definitions (34)–(36), the constraints with matrixes, (37)–(42) are obtained:

$$[P_{\min}] = [P_{1,\min} \quad P_{2,\min} \quad \dots \quad P_{N,\min}]^T \quad (34)$$

$$[P_{\max}] = [P_{1,\max} \quad P_{2,\max} \quad \dots \quad P_{N,\max}]^T \quad (35)$$

$$[P_{\min}] \leq [P] \leq [P_{\max}] \quad (36)$$

$$\left[\frac{\delta F_i(P_i)}{\delta P_i} \right] = [A_\lambda] \cdot [P_\lambda] + [B_\lambda] = 0 \quad (37)$$

$$\left[\frac{\delta F_i(P_i)}{\delta P_i} \right] = [A_\lambda] \cdot [P_\lambda] + [B_\lambda] < 0 \quad (38)$$

$$\left[\frac{\delta F_i(P_i)}{\delta P_i} \right] = [A_\lambda] \cdot [P_\lambda] + [B_\lambda] > 0 \quad (39)$$

$$[A_\lambda] = \begin{pmatrix} 2 \cdot H_{1,2} \cdot FC_1 & & 0 \\ & \ddots & \\ 0 & & 2 \cdot H_{N,2} \cdot FC_N \end{pmatrix} \quad (40)$$

$$[L_\lambda] = [\lambda \quad \lambda \quad \dots \quad \lambda]^T \quad (41)$$

$$[B_\lambda] = [L_\lambda] - [B(1:N)] \quad (42)$$

Solution $[L_\lambda]$ gives the incremental cost vector for N thermal units, the generated powers are in $[P_\lambda]$, (43) and (44), the operational costs in $F([P_\lambda])$, (45), and the total minimal operational cost F_λ are in (46):

$$[P_\lambda] = [P_{1\lambda} \quad P_{2\lambda} \quad \dots \quad P_{N\lambda}]^T \quad (43)$$

$$[P_\lambda] = [A_\lambda]^{-1} \cdot [B_\lambda] \quad (44)$$

$$F([P_\lambda]) = [H([P_\lambda])] \cdot [FC] \quad (45)$$

$$F_\lambda = \sum_{i=1}^N F([P_\lambda]) \quad (46)$$

The incremental costs $\frac{\delta F_i(P_i)}{\delta P_i}$ for final $[L_\lambda]$ and $[P_\lambda]$ are computed from (37). The total minimal cost for the hybrid thermosolar power plant, is computed from (47):

$$F_{opt} = \sum_{i=1}^N F([P_\lambda]) + t_s \cdot P_s \quad (47)$$

The software for solving the optimal hybrid thermosolar EDC problem, with λ iterations, (22)–(47), is programmed in Matlab. The data and parameters for 24 h are:

- Fixed data for generating units: characteristics of heat rates, number and rates of thermal units, prices of fuels, power bounds constraints, solar irradiation data, and load demand data.
- Parameter for accuracy of the results is the size of increment $\Delta\lambda$.

4. Study Case: Thermosolar System in North-West Greece

In this considered study case, the power system has seven thermal units, a CSP, a constant load at 1150 MW and a varying load demand ≤ 2 MW, as shown in Figure 2.

In Table A1, in Appendix A, are the ratings of seven thermal units located in the North-West Greece, Th1–Th7 selected from [66]: the generators' powers maximum limits, minimum limits, the heat consumption rates, and the costs rate of lignite. For all thermal units the heat/hour is a convex function with coefficients as specified in Equations (26) and (27). The cost rate is computed according to (28). The cost rate functions of the seven thermal units Th1–Th7 versus generated power are shown in Figure 3.

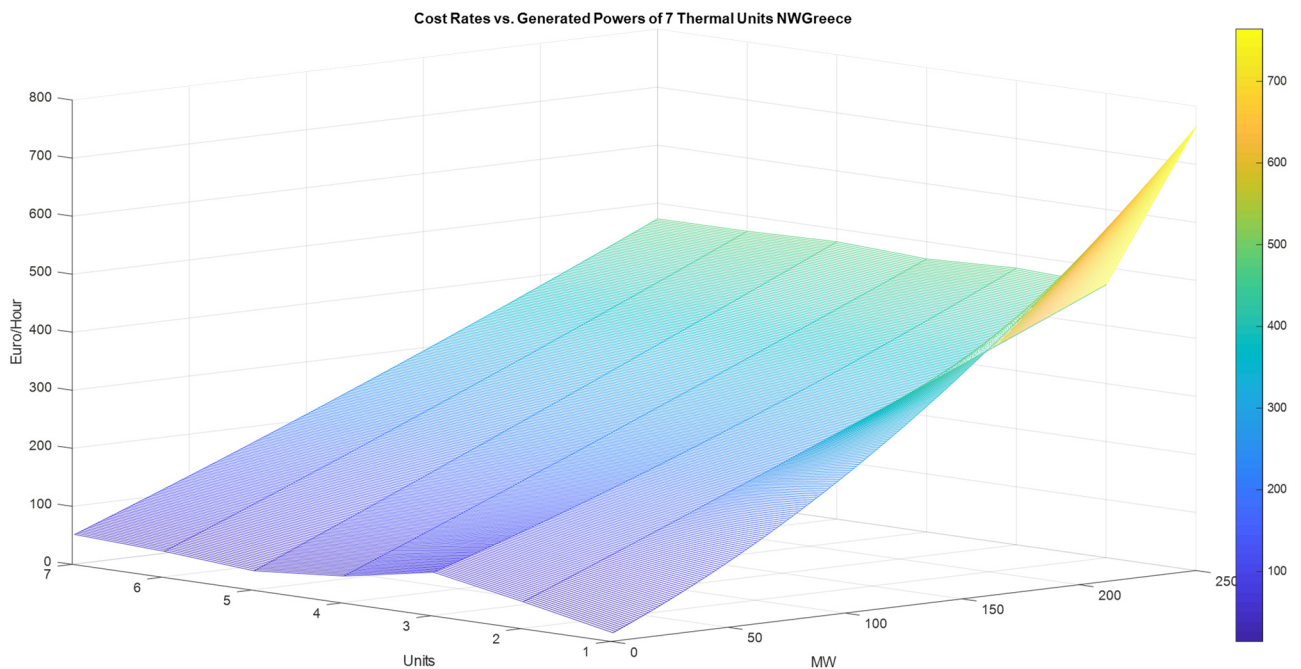


Figure 3. Cost rate functions versus generated power of seven thermal units from northwest Greece.

In Table A2, in Appendix A, are the technical data of the CSP unit [67]. In Table A3 in Appendix A are economic data of the solar field CSP unit [67].

First, are computed the unconstrained optimal solutions of the hybrid thermosolar system and are obtained the small displacements λ of the unconstrained optimal, varying from $\lambda_1 = 176.95$ to $\lambda_1 = 176.18$. Then, are computed the small displacements of λ and of the constrained optimal varying from $\lambda_\lambda = 175.95$ to $\lambda_\lambda = 174.71$. The generated powers by Th1–Th7, and the generated reserves of power, versus λ are plotted in Figure 4. The convergence of λ , beginning from the unconstrained optimal solution $[P_0]$, up to the constrained optimal solution $[P_\lambda]$, is also depicted in Figure 4. In Figure 5 are the constrained minimal cost generated powers $[P_\lambda]$, by the thermal units Th1–Th7, and by the CSP, from $\lambda_\lambda = 175.95$ to $\lambda_\lambda = 174.71$, over 24 h.

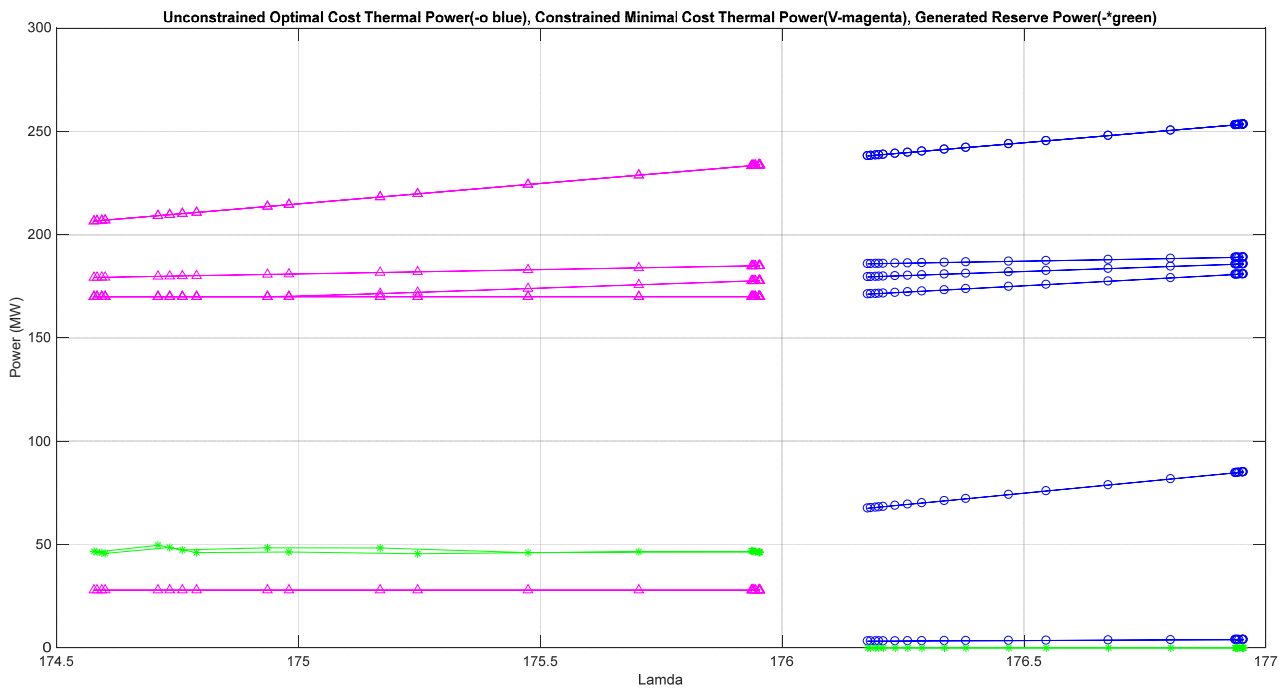


Figure 4. Convergence from unconstrained optimal cost to constrained optimal cost for the thermal units Th1–Th7 from northwest Greece over 24 h. The unconstrained minimal cost powers (blue o), the constrained minimal cost powers (magenta ∇), and the generated reserves of power (green*) are shown versus λ . Over 24 h, small displacements of unconstrained optimal λ , are varying from $\lambda_1 = 176.95$ to $\lambda_1 = 176.18$, and of constrained optimal λ_λ are varying from $\lambda_\lambda = 175.95$ to $\lambda_\lambda = 174.71$.

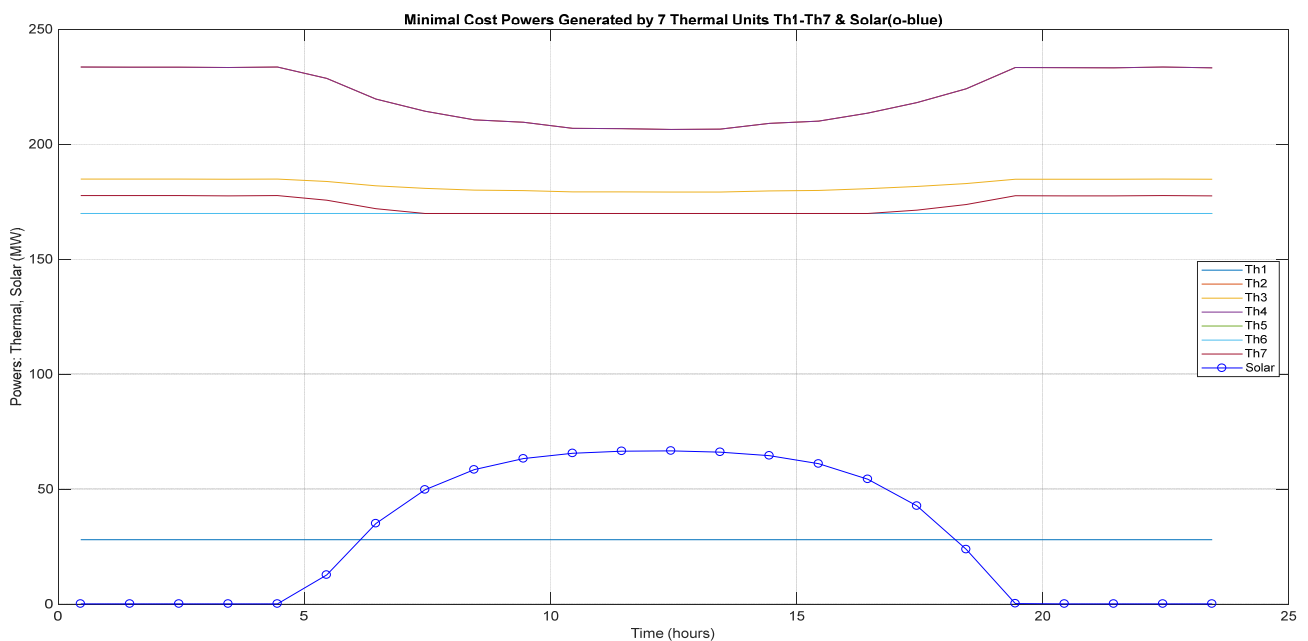


Figure 5. Constrained minimal cost generated powers [P_λ] by thermal units Th1–Th7 and solar power CSP unit from $\lambda_\lambda = 175.95$ to $\lambda_\lambda = 174.71$, over 24 h. The outputs of Th2 and Th4 are equal (shown superposed). The outputs of Th5 and Th6 are equal as well (superposed). The output of Th7 is equal to Th5 and Th6 between hours 6:45–17:45 (partly superposed).

5. Results, Discussion

In the following, two scenarios are studied and discussed: in Scenario 1, the hybrid thermosolar system composed of thermal Th1–Th7 with solar CSP enabled, and in Scenario 2, the thermal system of Th1–Th7 with CSP disabled. For carrying out the comparison between the two scenarios: hybrid Th1–Th7 with CSP enabled, and thermal Th1–Th7 with CSP disabled, are used the same data and parameters: the input data of the thermal units, the input data of the CSP system, the varying load demand, as presented previously, and in Appendix A, as well. The outputs of Th2 and Th4 are equal (shown superposed). The outputs of Th5 and Th6 are equal as well (superposed). The output of Th7 is equal to Th5 and Th6 between hours 6:45–17:45 (partly superposed).

In Figure 6a,b are plotted the unconstrained minimal costs, and the constrained minimal cost, respectively, for small displacements of λ over 24 h (Scenario1), where the CSP is shown as power unit 1 and Th1–Th7 as power units 2–8. The solution for Scenario 2, the same EDC problem of the same system, with the same thermal units Th1–Th7, and varying electric loads, but with CSP disabled, was computed, and the plots are shown in Figure 7a,b, for both unconstrained and constrained minimal costs, respectively.

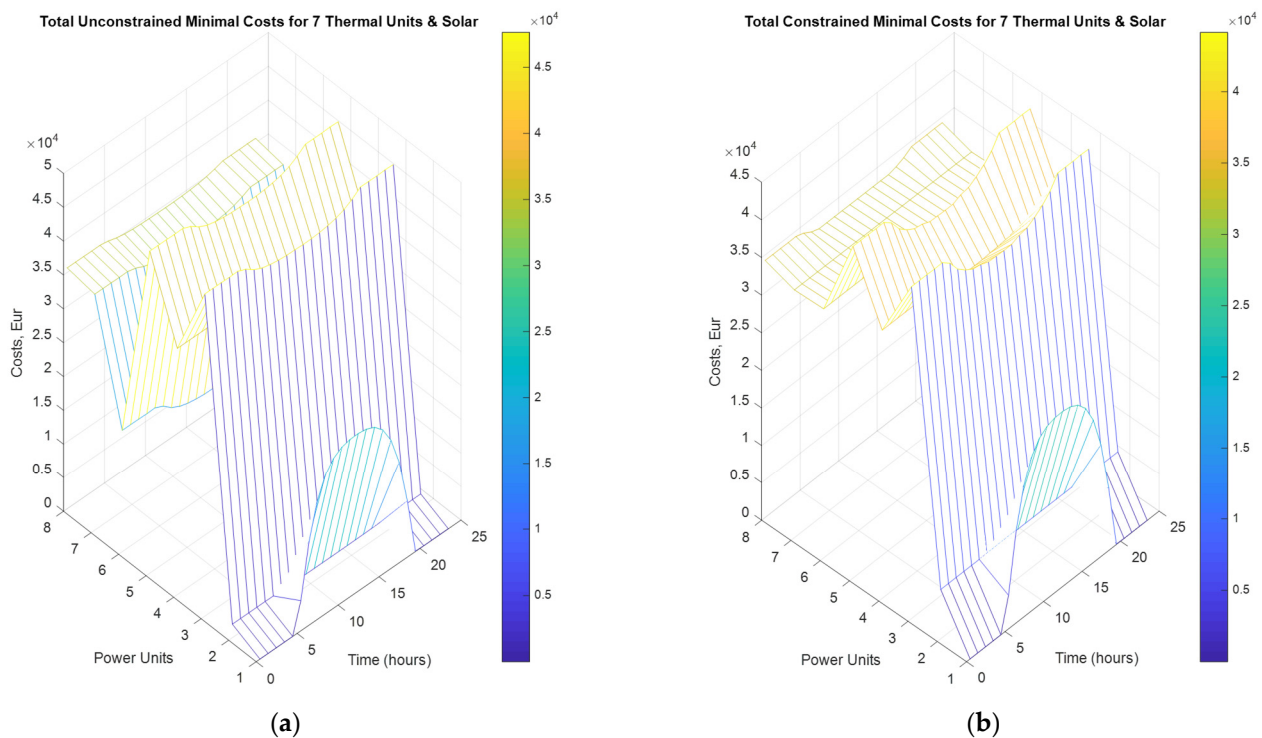


Figure 6. (a) Scenario 1: Total unconstrained minimal costs of seven thermal units and CSP over 24 h (CSP enabled); (b) Scenario 1: Total constrained minimal costs of seven thermal units and CSP over 24 h (CSP enabled).

From Figure 6a,b and Figure 7a,b it is clearly shown that, in situations when CSP is disabled, related to the variability of solar irradiation, the thermal units Th1–Th7 increase production to compensate for the missing amount of generation from CSP and to balance the load demands, without the need for batteries or energy storage.

Figure 8 shows the balance of generated powers during Scenario 1, by hybrid thermosolar with CSP enabled system, of an optimally constrained thermal system, of generated reserves, versus total varying electric load, over 24 h.

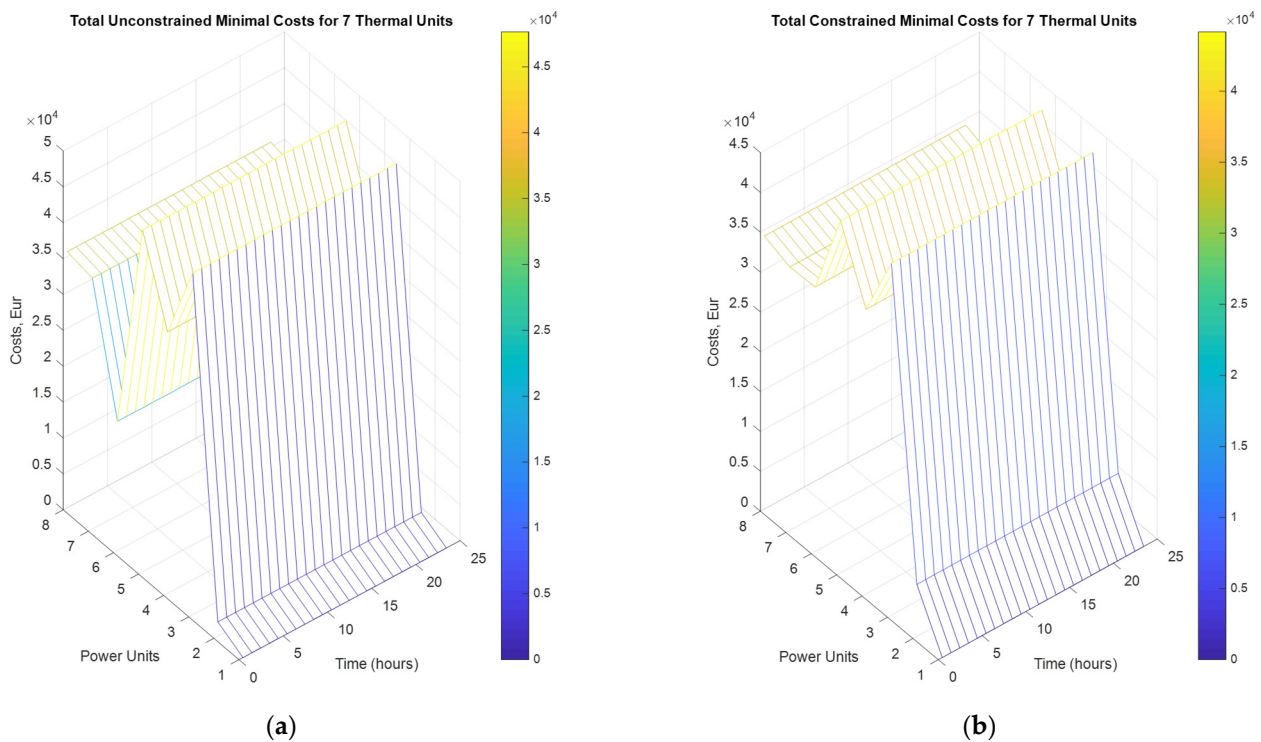


Figure 7. (a) Scenario 2: Total unconstrained minimal costs of seven thermal units over 24 h (CSP disabled); (b) Scenario 2: Total constrained minimal costs of seven thermal units over 24 h (CSP disabled).

Balance of Powers with CSP enabled

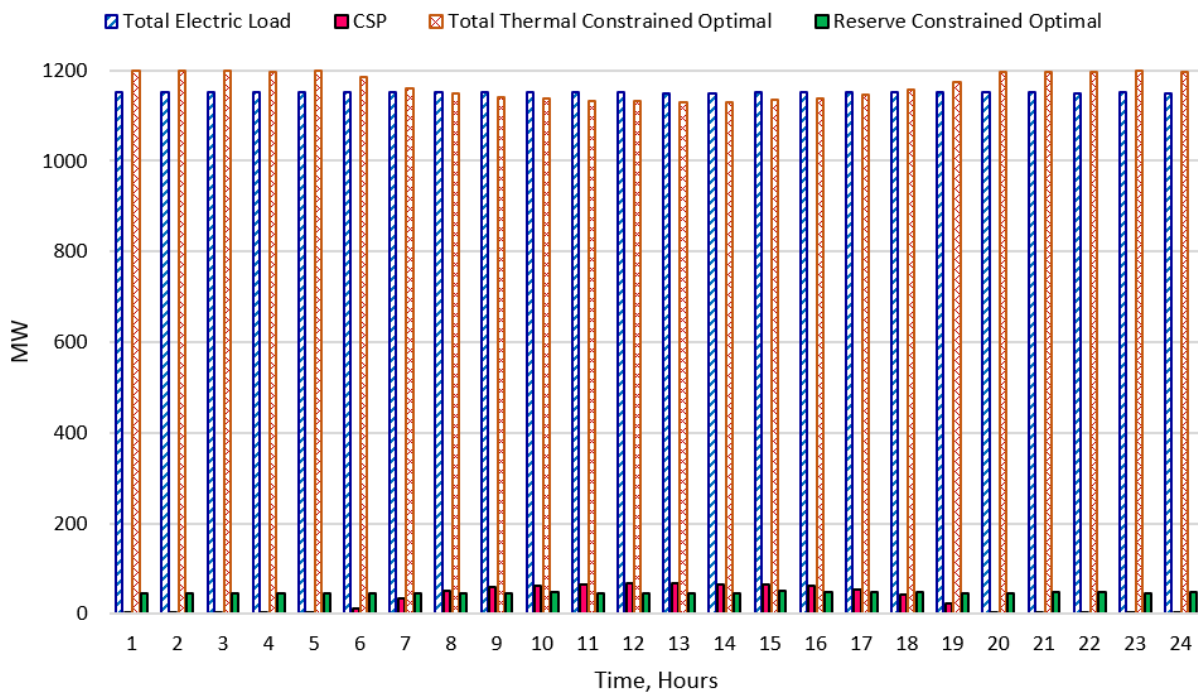


Figure 8. Scenario 1: The balance of generated powers of optimally constrained hybrid thermosolar system, of generated reserves, with total varying electrical load, during 24 h (CSP enabled).

In Figure 9 is the balance of powers for the two scenarios: in Scenario 1, hybrid thermosolar with CSP enabled and in Scenario 2, thermal with CSP disabled.

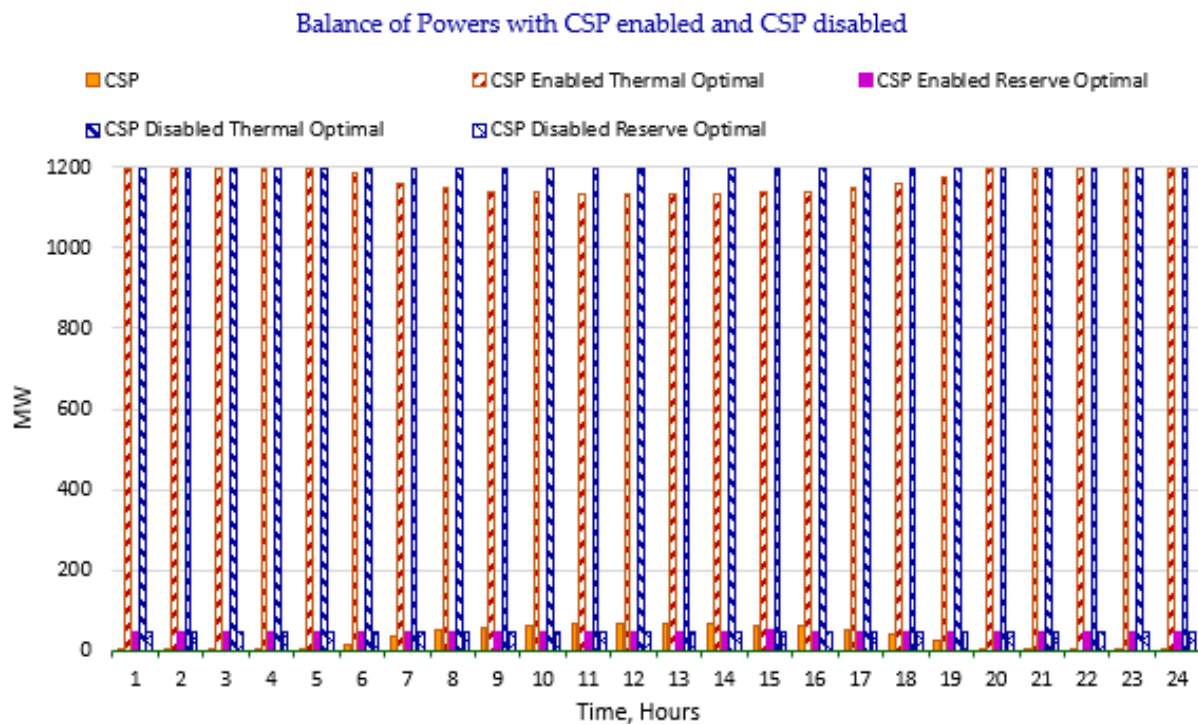


Figure 9. Balance of powers in Scenario 1 (hybrid system with CSP enabled) and Scenario 2 (thermal system with CSP disabled), during 24 h.

In Scenario 2, when CSP is disabled, the thermal units Th1–Th7 undertake to generate the total requested power to balance the load demand. In this context, in both scenarios, Th1, Th5, and Th6 generate at $P_{1,\min}$, $P_{5,\min}$, and $P_{6,\min}$, respectively. The other four thermal units, Th2, Th3, Th4 and Th7 increase production to compensate for the amount of MW missing by disabling the CSP. This process can be seen in Table 1.

Table 1 shows the numerical results obtained using this integrated approach, for both Scenarios 1 and 2 and varying load demands over 24 h. The results of Scenario 2 (thermal units only, CSP disabled) are marked with the subscript *ref*. Specifically, for Scenario 1, (hybrid thermosolar with Th1–Th7 and CSP enabled) are the columns titled “Total Generated Energy (MWh) E_i ”, and “Total Operational Costs F_i ”. The values computed for Scenario 2 (thermal units only, CSP disabled) are in the columns titled “Total Generated Energy (MWh) $E_{i,ref}$ ” and “Total Operational Costs $F_{i,ref}$ ”. The two sets of results from Scenarios 1 and 2 are compared, and the results are shown in the column “Differences Scenario 1–Scenario 2” from enabling to disabling the CSP in power generation and optimization of costs.

The results in Table 1 show that thermal units Th1, Th5, and Th6 generate at minimum power $P_{i,\min}$, over 24 h and are not influenced by enabling or disabling the CSP. Thermal units Th2, Th3, and Th4 function at levels $P_{i,\min} \leq P_i \leq P_{i,\max}$.

In Scenario 1, unit Th7 functions at $P_{7,\min}$ between hours 6:45–17:45 (with sunshine) and at levels $P_{7,\min} \leq P_7 \leq P_{7,\max}$ during the hours of the day 0:45–6:45 and 17:45–23:45 (without sunshine). Operation of Th7 at $P_{7,\min}$ during sunshine is saving CO₂ emissions.

None of the thermal units Th1–Th7 function at maximum power $P_{i,\max}$ and this fact adds more savings to CO₂ emissions.

Table 1. Total Generated Energy and Total Operational Costs over 24 h.

Thermal Units	Scenario 1 CSP Enabled			Scenario 2 CSP Disabled			Differences: Scenario 1–Scenario 2	
	Constraints—Boundary Values	Total Generated Energy (MWh)	Total Operational Costs (EUR)	Constraints—Boundary Values	Total Generated Energy (MWh)	Total Operational Costs (EUR)	Total Generated Energy (MWh)	Total Operational Costs (EUR)
		E_i	F_i		$E_{i,ref}$	$F_{i,ref}$	$E_i - E_{i,ref}$	$F_i - F_{i,ref}$
Th1	$P_1 = P_{1,min}$	672.00	156,480	$P_1 = P_{1,min}$	672.00	156,480	0	0
Th2	$P_{2,min} \leq P_2 \leq P_{2,max}$	5321.77	1,009,361	$P_{2,min} \leq P_2 \leq P_{2,max}$	5606.49	1,059,295	−284.73	−49,934
Th3	$P_{3,min} \leq P_3 \leq P_{3,max}$	4378.62	846,277	$P_{3,min} \leq P_3 \leq P_{3,max}$	4437.97	856,686	−59.35	−10,409
Th4	$P_{4,min} \leq P_4 \leq P_{4,max}$	5321.77	1,009,361	$P_{4,min} \leq P_4 \leq P_{4,max}$	5606.49	1,059,295	−284.73	−49,934
Th5	$P_5 = P_{5,min}$	4080.00	796,330	$P_5 = P_{5,min}$	4080.00	796,330	0	0
Th6	$P_6 = P_{6,min}$	4080.00	792,694	$P_6 = P_{6,min}$	4080.00	792,694	0	0
Th7	0:45–6:45 and 17:45–23:45: $P_{7,min} \leq P_7 \leq P_{7,max}$ 6:45–17:45: $P_7 = P_{7,min}$	4170.17	805,430	$P_{7,min} \leq P_7 \leq P_{7,max}$	4265.17	822,102	−95.00	−16,673
CSP	-	731.34	255,969	-	0	0	731.34	255,969
Totals		28,755.67	5,671,901		28,748.13	5,542,882	7.54	129,019

Table 2 shows that the mean minimal operational cost of the hybrid thermosolar system is at 8.22 EUR/MW (Scenario 1) and it is higher than the mean minimal operational cost of the thermal system at 8.03 EUR/MW (Scenario 2). Thus, the cost of 1 MW generated by hybrid thermosolar at 8.22 (EUR/MW) is higher than the cost of 1 MW generated by the thermal system with lignite at 8.03 (EUR/MW).

Respectively, the cost of 1 MWh is higher when generated by the hybrid thermosolar system in Scenario 1, at the 197.24 EUR/MWh, than by the thermal system in Scenario 2, at the 192.81 EUR/MWh.

From the above comparison results it is clear that, the operational cost of coal-based production of electrical energy is lower than the operational cost for the production of electrical energy from the hybrid thermosolar system, and, that the combination of coal with solar energy increases the minimal cost per 1 MW, and per 1MWh, as compared to the production from coal only. The increased cost of energy produced by the hybrid thermosolar system can be partly balanced by the generated reserves of MW, see Figures 4, 8 and 9.

However, the costs of MWh, and MW produced by CSP alone are higher than the costs of MWh, and MW produced by the hybrid system, Table 2. Also, they are higher than the costs of MWh and of MW produced from fossil fuels only.

Table 2. Mean Minimal Operational Costs per MW.

Thermal Units	Scenario 1 CSP Enabled		Scenario 2 CSP Disabled		Differences Scenario 1–Scenario 2	
	Mean Operational Costs per 1 MWh (EUR/MWh)	Mean Operational Costs per 1 MW (EUR/MW)	Mean Operational Costs per MWh (EUR/MWh)	Mean Operational Costs per 1 MW (EUR/MW)	Mean Operational Costs per MWh (EUR/MWh)	Mean Operational Costs per 1 MW (EUR/MW)
	F_i/E_i	$F_i/E_i/h$	$F_{i,ref}/E_{i,ref}$	$F_{i,ref}/E_{i,ref}/h$	$F_i/E_i - F_{i,ref}/E_{i,ref}$	$F_i/E_i/h - F_{i,ref}/E_{i,ref}/h$
Th1	232.86	9.70	232.86	9.70	0	0
Th2	189.67	7.90	188.94	7.87	0.73	0.03
Th3	193.27	8.05	193.04	8.04	0.24	0.01
Th4	189.67	7.90	188.94	7.87	0.73	0.03
Th5	195.18	8.13	195.18	8.13	0	0

Table 2. Cont.

Thermal Units	Scenario 1 CSP Enabled		Scenario 2 CSP Disabled		Differences Scenario 1–Scenario 2	
	Mean Operational Costs per 1 MWh (EUR/MWh)	Mean Operational Costs per 1 MW (EUR/MW)	Mean Operational Costs per MWh (EUR/MWh)	Mean Operational Costs per 1 MW (EUR/MW)	Mean Operational Costs per MWh (EUR/MWh)	Mean Operational Costs per 1 MW (EUR/MW)
	F_i/E_i	$F_i/E_i/h$	$F_{i,ref}/E_{i,ref}$	$F_{i,ref}/E_{i,ref}/h$	$F_i/E_i - F_{i,ref}/E_{i,ref}$	$F_i/E_i/h - F_{i,ref}/E_{i,ref}/h$
Th6	194.29	8.10	194.29	8.10	0	0
Th7	193.14	8.05	192.75	8.03	0.39	0.02
CSP	350.00	14.58	0	0	350.00	14.58
Totals	197.24	8.22	192.81	8.03	4.44	0.18

6. Conclusions

The new knowledge from this integrated approach for EDC optimization applied to thermosolar CSP systems consists of the followings:

This work advances prior knowledge with an integrated model, based on exact mathematics of matrices and solutions, which offers access to researchers, working in techno-economic fields, to solve EDC problems for thermosolar generators. This approach optimizes costs of the hybrid energy-generating systems with large numbers of power units, boundary operating zones, boundary conditions, with different fuels and unit prices.

The algorithm determines the global optimal solution for incremental cost of the unconstrained optimal EDC problem, and considers it as the starting point for the initial value for solving the constrained optimal EDC. From the constrained optimal operating point, the algorithm finds the generating units which are set to minimum power, and the generating units which will operate between the limits of minimum and maximum power generation. The constrained minimal total operational cost is deducted with accuracy, and depends on parameters of thermal units, fuel costs, varying load demand, power bound conditions, power balance, and solar CSP parameters.

The study case of the hybrid thermosolar system resulted as a consequence of CSP operation, in three of the seven thermal units being set to the minimum power generating limit, while, at the same time, no thermal power unit was set to the maximum power generating limit, and, thus, the CO₂ emissions were diminished.

In conclusion, the cost of fuel influences the final minimal operational cost of generated electrical energy and power; the introduction of hybrid thermosolar leads to increased costs if compared to fossil fuel generation. Thus, to acquire the benefits of cleaner electrical energy with diminished emissions versus the minimal costs of electrical energy generation belongs to multicriteria managerial decisions.

This work contributes to increasing energy literacy. This will support researchers in studying EDC problems by applying multidisciplinary knowledge, information, and multicriteria managerial decisions, to mathematically solve energy-economic problems.

Funding: This research received no external funding.

Institutional Review Board Statement: Not applicable.

Informed Consent Statement: Not applicable.

Data Availability Statement: Not applicable.

Conflicts of Interest: The author declares no conflict of interest.

Appendix A

In Table A1 are the ratings of seven thermal units from the Northwest Greek power system, the constraints the coefficients of heat consumption rates, and the locations of thermal units, selected from [66]. The cost rate for lignite is selected at 100.00 EUR/Gcal.

In Table A2 are the technical data of one solar field concentrating solar power CSP [67], selected because latitude location is close to Ptolemaida. In Table A3 are the economic data of the same solar field CSP unit from Table A2 [67].

Table A1. Ratings of Seven Thermal Units in North-West of Greece.

Thermal Units	$P_{i,\min}$ (MW)	$P_{i,\max}$ (MW)	Heat Consumption Rates			Locations
			$H_{i,2}$	$H_{i,1}$	$H_{i,0}$	
Th1	28	70	0.005102	1.7286	12.80	Ptolemaida I
Th2	120	300	0.000254	1.6410	44.19	Ptolemaida IV
Th3	120	300	0.001217	1.3095	73.20	Kardia III–IV
Th4	120	300	0.000254	1.6410	44.19	Kardia I–II
Th5	170	300	0.000222	1.7318	30.99	Agios Dimitrios I–II
Th6	170	310	0.000399	1.6253	42.47	Agios Dimitrios III–IV
Th7	170	300	0.000622	1.5386	49.49	Amidaio I–II
Totals	898	1880				

Table A2. Technical data of Solar Field CSP.

Technology	Hybrid, Parabolic Trough
Power Cycle	Steam Rankine
Nominal Capacity (MW)	22.5
Turbine efficiency %	37
Expected Generation (GWh/year)	44.1
Latitude/Longitude Location (°)	41.529/0.8
Solar Field Aperture Area (m ²)	183120
Number of Solar Collector Assemblies (SCAs)	336
Number of Loops	56
Number of SCAs per Loop	6
Number of Modules per SCA	8
SCA Aperture Area (m ²)	545
SCA Length (m)	96

Table A3. Economic data of Solar Field CSP.

Total Construction Cost (2012) M EUR	149.94
Total Cost (2020) M EUR	211.67
Specific Cost (2020) EUR/kW	9407.41
Remuneration EUR/kWh	0.27
Remuneration Start Year	2012
Remuneration Deflated (2020) EUR/kWh	0.37

Table A3. Cont.

PPA or Tariff Period (Years)	25
Operation and Maintenance O/M (%) (% of investment cost per year)	1.5
Levelized Cost of Electricity (2020) EUR/kWh (LCOE with 5% weighted average cost of capital and 25-year payback period)	0.41

References

- Harsem, T.T.; Nourozi, B.; Behzadi, A.; Sadrizadeh, S. Design and Parametric Investigation of an Efficient Heating System, an Effort to Obtain a Higher Seasonal Performance Factor. *Energies* **2021**, *14*, 8475. [CrossRef]
- Stamatakis, M.E.; Ioannides, M.G. State Transitions Logical Design for Hybrid Energy Generation with Renewable Energy Sources in LNG Ship. *Energies* **2021**, *14*, 7803. [CrossRef]
- Ladakakos, P.D.; Ioannides, M.G.; Vionis, P.S.; Fragoulis, A.N. Development of a simulation model for investigating the dynamic operation of autonomous wind-diesel system. In Proceedings of the 7th European Wind Energy Conference EWEC-1997, Dublin, Ireland, 6–9 October 1997; European Wind Energy Association: Brussels, Belgium, 1997; pp. 833–836.
- Papazis, S.A.; Ioannides, M.G.; Fotilas, P.N. An Information System for Multiple Criteria Assessment of Renewable Energy Power Plants. *Wind Eng.* **2000**, *24*, 81–99. [CrossRef]
- Gayme, D.; Topcu, U. Optimal power flow with large-scale storage integration. *IEEE Trans. Power Syst.* **2012**, *28*, 709–717. [CrossRef]
- IRENA. *Renewable Power Generation Costs in 2021*; International Renewable Energy Agency: Abu Dhabi, United Arab Emirates, 2022; ISBN 978-92-9260-452-3. Available online: <https://www.irena.org/publications/2022/Jul/Renewable-Power-Generation-Costs-in-2021> (accessed on 16 July 2022).
- CNN.gr. 2022. Available online: <https://fox24.gr/2022/07/09/dimioyrgeitai-neo-ergostasio-lignit/> (accessed on 9 July 2022).
- Conejo, A.J.; Baringo, L. *Power System Operations*; Springer International Publishing AG: Cham, Switzerland, 2018; pp. 197–216. [CrossRef]
- Wood, A.J.; Wollenbeg, B.F.; Sheble, G.B. *Power Generation, Operation and Control*, 3rd ed.; Wiley: Hoboken, NJ, USA, 2014.
- Papazis, S.A.; Bakos, G.C. Generalized Model of Economic Dispatch Optimization as an Educational Tool for Management of Energy Systems. *Adv. Electr. Comput. Eng.* **2021**, *21*, 75–86. [CrossRef]
- García, J.M.G.-V.; García-Carmona, M.; Trujillo Torres, J.M.; Moya-Fernández, P. Teacher Training for Educational Change: The View of International Experts. *Contemp. Educ. Technol.* **2022**, *14*, ep330. [CrossRef]
- Klaassen, R.; de Vries, P.; Ioannides, M.G.; Papazis, S.A. Tipping your toe in the ‘Emerging Technologies’ pond from an educational point of view. In Proceedings of the 45th SEFI Annual Conference 2017—Education Excellence for Sustainability, SEFI 2017, Azores, Portugal, 18–21 September 2017; pp. 1190–1197. Available online: <https://www.sefi.be/proceedings/?conference=2017-azores> (accessed on 17 July 2022).
- Ioannides, M.G.; Papazis, S.A. Teaching and Research in Emerging Electrical Energy Engineering Education. In Proceedings of the 2021 International Conference on Applied and Theoretical Electricity (ICATE), Craiova, Romania, 27–29 May 2021; pp. 1–5. [CrossRef]
- Papazis, S.A.; Ioannides, M.G. Emerging Energy Engineering Education on the Way to Employment. In *Learning with Technologies and Technologies in Learning*; Auer, M.E., Pester, A., May, D., Eds.; Lecture Notes in Networks and Systems, 456; Springer Nature: Cham, Switzerland, 2022; pp. 655–677. [CrossRef]
- Fotilas, P.N.; Papazis, S.A. A multiple criteria decision support system for the assessment of renewable energy power plants. In Proceedings of the 3rd International Symposium on Advanced Electromechanical Motion Systems, Electromotion, Patras, Greece, 8–9 July 1999; Volume 2, pp. 921–927.
- Ladakakos, P.D.; Ioannides, M.G. Estimation of wind parameter variation effect on the power quality of hybrid weak grids. *Wind Eng.* **1999**, *23*, 353–364. Available online: <https://www.jstor.org/stable/43749905> (accessed on 17 July 2022).
- Papazis, S.A.; Ioannides, M.G.; Fotilas, P.N. Development of an Information System for Wind Power Stations. In *Enterprise Information Systems II*; Sharp, B., Filipe, J., Cordeiro, J., Eds.; Springer: Dordrecht, The Netherlands, 2001; pp. 101–107. [CrossRef]
- Ioannides, M.G.; Tuduce, R.; Cristea, P.-D.; Papazis, S.A. Wind power generating systems based on double output induction machine: Considerations about control techniques. In Proceedings of the 20th International Conference on Systems, Signals and Image Processing (IWSSIP), Bucharest, Romania, 7–9 July 2013; pp. 103–107. [CrossRef]
- Ioanides, M.G.; Stamelos, A.; Papazis, S.A.; Papoutsidakis, A.; Vikentios, V.; Apostolakis, N. IoT Monitoring System for Applications with Renewable Energy Generation and Electric Drives. *Renew. Energy Power Qual. J.* **2021**, *19*, 565–570. [CrossRef]
- Østergaard, P.A.; Duic, N.; Noorollahi, Y.; Kalogirou, S.A. Latest progress in Sustainable Development using renewable energy technology. *Renew. Energy* **2020**, *162*, 1554–1562. [CrossRef]
- Østergaard, P.A.; Duic, N.; Noorollahi, Y.; Mikulcic, H.; Kalogirou, S. Sustainable development using renewable energy technology. *Renew. Energy* **2020**, *146*, 2430–2437. [CrossRef]

22. Østergaard, P.A.; Duic, N.; Noorollahi, Y.; Kalogirou, S.A. Recent advances in renewable energy technology for the energy transition. *Renew. Energy* **2021**, *179*, 877–884. [[CrossRef](#)]
23. Chen, Q.; Wang, Y.; Zhang, J.; Wang, Z. The Knowledge Mapping of Concentrating Solar Power Development Based on Literature Analysis Technology. *Energies* **2020**, *13*, 1988. [[CrossRef](#)]
24. Bakos, G.C.; Papazis, S.A. Solar Aided Power Generation (SAPG) System Using Parabolic Troughs: Techno-Economic Scenarios. In Proceedings of the 3rd International Conference on Advances in Energy Research and Applications (ICAERA'22), Seoul, Korea, 27–29 October 2022; Paper No. 102. pp. 1–5.
25. Maffezzoni, P.; Codecasa, L.; D'Amore, D. Modeling and Simulation of a Hybrid Photovoltaic Module Equipped with a Heat-Recovery System. *IEEE Trans. Ind. Electron.* **2009**, *56*, 4311–4318. [[CrossRef](#)]
26. Rehman, A.U.; Wadud, Z.; Elavarasan, R.M.; Hafeez, G.; Khan, I.; Shafiq, Z.; Alhelou, H.H. An Optimal Power Usage Scheduling in Smart Grid Integrated with Renewable Energy Sources for Energy Management. *IEEE Access* **2021**, *9*, 84619–84638. [[CrossRef](#)]
27. Kalogirou, S.; Lloyd, S.; Ward, J.; Eleftheriou, P. Design and performance characteristics of a parabolic-trough solar-collector system. *Appl. Energy* **1994**, *47*, 341–354. [[CrossRef](#)]
28. Montes, M.; Abánades, A.; Martínez-Val, J. Performance of a direct steam generation solar thermal power plant for electricity production as a function of the solar multiple. *Sol. Energy* **2009**, *83*, 679–689. [[CrossRef](#)]
29. Ranjan, S.; Chandra Das, D.; Latif, A.; Sinha, N.; Suhail Hussain, S.M.; Selim Ustun, T. Maiden Voltage Control Analysis of Hybrid Power System with Dynamic Voltage Restorer. *IEEE Access* **2021**, *9*, 60531–60542. [[CrossRef](#)]
30. Valenzuela, L.; Zarza, E.; Berenguel, M.; Camacho, E. Control scheme for direct steam generation in parabolic troughs under recirculation operation mode. *Sol. Energy* **2006**, *80*, 1–17. [[CrossRef](#)]
31. López-Álvarez, J.A.; Larrañeta, M.; Pérez-Aparicio, E.; Silva-Pérez, M.A.; Lillo-Bravo, I. An Approach to the Operation Modes and Strategies for Integrated Hybrid Parabolic Trough and Photovoltaic Solar Systems. *Sustainability* **2021**, *13*, 4402. [[CrossRef](#)]
32. Poullikkas, A. Economic analysis of power generation from parabolic trough solar thermal plants for the Mediterranean region—A case study for the island of Cyprus. *Renew. Sustain. Energy Rev.* **2009**, *13*, 2474–2484. [[CrossRef](#)]
33. Riahi, A.; Haj Ali, A.B.; Guizani, A.; Balghouthi, M. Performance study of a concentrated photovoltaic thermal hybrid solar system. In Proceedings of the 2019 10th International Renewable Energy Congress (IREC), Sousse, Tunisia, 26–28 March 2019; pp. 1–5. [[CrossRef](#)]
34. ASHRAE American Society of Heating, Refrigerating, and Air-Conditioning Engineers. *Standard Method of Testing to Determine the Thermal Performance of Solar Collectors*; U.S. Department of Energy, Office of Scientific Technical Information: Oak Ridge, TN, USA, 1991.
35. Bouhal, T.; Agrouaz, Y.; Kousksou, T.; Jamil, A.; Zeraouia, Y.; El-Rhafiki, T.; Bakkas, M. CSP plants optimization in Morocco: Best practices and real challenges. In Proceedings of the 2016 International Renewable and Sustainable Energy Conference (IRSEC), Marrakesh, Morocco, 17 November 2016; pp. 269–274. [[CrossRef](#)]
36. Kannaiyan, S.; Bokde, N.D.; Geem, Z.W. Solar Collectors Modeling and Controller Design for Solar Thermal Power Plant. *IEEE Access* **2020**, *8*, 81425–81446. [[CrossRef](#)]
37. Mufti, G.M.; Jamil, M.; Naeem, D.; Mukhtiar, M.U.; Al-Awami, A.T. Performance analysis of parabolic trough collectors for Pakistan using mathematical and computational models. In Proceedings of the 2016 Clemson University Power Systems Conference (PSC), Clemson, SC, USA, 8–11 March 2016; pp. 1–8. [[CrossRef](#)]
38. Shabbir, N.S.K.; Alam Chowdhury, M.S.; Liang, X. A Guideline of Feasibility Analysis and Design for Concentrated Solar Power Plants. *Can. J. Electr. Comput. Eng.* **2018**, *41*, 203–217. [[CrossRef](#)]
39. Valan-Arasu, A.; Sornakumar, T. Theoretical analysis and experimental verification of parabolic trough solar collector with hot water generation system. *Therm. Sci.* **2007**, *11*, 119–126. [[CrossRef](#)]
40. Zaaoumi, A.; Bouramdane, Z.; Bah, A.; Alaoui, M.; Mechaqrane, A. Energy production estimation of a parabolic trough solar power plant using artificial neural network. In Proceedings of the 2020 International Conference on Electrical and Information Technologies (ICEIT), Rabat-Salé, Morocco, 4–7 March 2020; pp. 1–6. [[CrossRef](#)]
41. Bentouba, S.; Bourouis, M. Feasibility study of a wind-photovoltaic hybrid power generation system for a remote area in the extreme south of Algeria. *Appl. Therm. Eng.* **2016**, *99*, 713–719. [[CrossRef](#)]
42. Karnavas, Y.L. The Autonomous Electrical Power System of Crete Island—A Review. *Int. Rev. Electr. Eng. Praise Ed.* **2006**, *1*, 1–8.
43. Bakos, G.; Tsechelidou, C. Solar aided power generation of a 300 MW lignite fired power plant combined with line-focus parabolic trough collectors' field. *Renew. Energy* **2013**, *60*, 540–547. [[CrossRef](#)]
44. Huang, C.; Madonski, R.; Zhang, Q.; Yan, Y.; Zhang, N.; Yang, Y. On the use of thermal energy storage in solar-aided power generation systems. *Appl. Energy* **2022**, *310*, 118532. [[CrossRef](#)]
45. Huang, C.; Hou, H.; Hu, E.; Liang, M.; Yang, Y. Impact of power station capacities and sizes of solar field on the performance of solar aided power generation. *Energy* **2017**, *139*, 667–679. [[CrossRef](#)]
46. Liu, H.; Zhai, R.; Patchigolla, K.; Turner, P.; Yang, Y. Model predictive control of a combined solar tower and parabolic trough aided coal-fired power plant. *Appl. Therm. Eng.* **2021**, *193*, 116998. [[CrossRef](#)]
47. Petrovic, R. Economic dispatching in power systems using optimal control theory. In *Optimization and Control of Dynamic Operational Research Models*; Tzafestas, S.G., Ed.; North-Holland Publishing: Amsterdam, The Netherlands, 1982; Volume 4, pp. 217–250.
48. Khare, V.; Nema, S.; Baredar, P. Solar wind hybrid renewable energy system: A review. *Renew. Sustain. Energy Rev.* **2016**, *58*, 23–33. [[CrossRef](#)]

49. Chen, C.; Wang, F.; Zhou, B.; Chan, K.W.; Cao, Y.; Tan, Y. An interval optimization-based day-ahead scheduling scheme for renewable energy management in smart distribution systems. *Energy Convers. Manag.* **2015**, *106*, 584–596. [[CrossRef](#)]
50. Reddy, S.S.; Momoh, J.A. Realistic and transparent optimum scheduling strategy for hybrid power system. *IEEE Trans. Smart Grid* **2015**, *6*, 3114–3125. [[CrossRef](#)]
51. Dike, D.; Adinfono, M.I.; Ogu, G. Economic Dispatch of Generated Power Using Modified Lambda-Iteration Method. *IOSR-JEEE J. Electr. Electron. Eng.* **2013**, *7*, 49–54. [[CrossRef](#)]
52. Han, X.; Gooi, H. Effective economic dispatch model and algorithm. *Int. J. Electr. Power Energy Syst.* **2007**, *29*, 113–120. [[CrossRef](#)]
53. Zhan, J.P.; Wu, Q.H.; Guo, C.X.; Zhou, X.X. Fast λ -Iteration Method for Economic Dispatch with Prohibited Operating Zones. *IEEE Trans. Power Syst.* **2013**, *29*, 990–991. [[CrossRef](#)]
54. Farag, A.; Al-Baiyat, S.; Cheng, T. Economic load dispatch multiobjective optimization procedures using linear programming techniques. *IEEE Trans. Power Syst.* **1995**, *10*, 731–738. [[CrossRef](#)]
55. Sinha, N.; Chakrabarti, R.; Chattopadhyay, P. Evolutionary programming techniques for economic load dispatch. *IEEE Trans. Evol. Comput.* **2003**, *7*, 83–94. [[CrossRef](#)]
56. Ding, T.; Bie, Z. Parallel augmented Lagrangian relaxation for dynamic economic dispatch using diagonal quadratic approximation method. *IEEE Trans. Power Syst.* **2017**, *32*, 1115–1126. [[CrossRef](#)]
57. Li, Z.; Wu, W.; Zhang, B.; Sun, H.; Guo, Q. Dynamic economic dispatch using Lagrangian relaxation with multiplier updates based on a quasi-Newton method. *IEEE Trans. Power Syst.* **2013**, *28*, 4516–4527. [[CrossRef](#)]
58. Solar Irradiance Calculations. 2022. Available online: https://re.jrc.ec.europa.eu/pvg_tools/en/tools.html (accessed on 30 June 2022).
59. Reddy, S.S.; Bijwe, P.R.; Abhyankar, A.R. Real-Time Economic Dispatch Considering Renewable Power Generation Variability and Uncertainty Over Scheduling Period. *IEEE Syst. J.* **2014**, *9*, 1440–1451. [[CrossRef](#)]
60. Chen, C.L.; Lee, T.Y.; Jan, R.M. Optimal wind-thermal coordination dispatch in isolated power systems with large integration of wind capacity. *Energy Convers. Manag.* **2006**, *47*, 3456–3472. [[CrossRef](#)]
61. Reddy, S.S. Optimal scheduling of thermal-wind-solar power system with storage. *Renew. Energy* **2017**, *101*, 1357–1368. [[CrossRef](#)]
62. Xie, L.; Chiang, H.D.; Li, S.H. Optimal power flow calculation of power system with wind farms. In Proceedings of the IEEE Power Energy Society General Meeting, Detroit, MI, USA, 24–29 July 2011; pp. 1–6.
63. Hetzer, J.; Yu, D.C.; Bhattarai, K. An economic dispatch model incorporating wind power. *IEEE Trans. Energy Convers.* **2008**, *23*, 603–611. [[CrossRef](#)]
64. Jabr, R.; Pal, B. Intermittent wind generation in optimal power flow dispatching. *IET Gener. Transm. Distrib.* **2009**, *3*, 66–74. [[CrossRef](#)]
65. Hoffmann, L.D.; Bradley, G.L. *Calculus for Business, Economics, and the Social and Life Sciences*, 10th ed.; McGraw Hill: New York, NY, USA, 2010; pp. 613–647. ISBN 978-0-07-353231-8.
66. Papanikolaou, D.N. Economic Operation of Power Systems. Master’s Thesis, University of Patras, Patras, Greece, 21 February 2008. Available online: <http://nemertes.lis.upatras.gr/jspui/handle/10889/725> (accessed on 11 August 2022). (In Greek).
67. Hybrid Parabolic Trough Projects. 2022. Available online: <https://solarpaces.nrel.gov/by-technology/hybrid-parabolic-trough> (accessed on 16 July 2022).